MULTI-LEVEL ANALYSIS OF LOCALISATION PROBLEMS

L.J. Sluys

Delft University of Technology, Faculty of Civil Engineering and Geosciences,
P.O. Box 5048, 2600 GA Delft, the Netherlands
e-mail: L.J.Sluys@citg.TUDelft.nl

Y. Estrin

Institut für Werkstoffkunde und Werkstofftechnik (IWW)
TU Clausthal, D-38678 Clausthal-Zellerfeld, Germany
e-mail: juri.estrin@tu-clausthal.de

G.N. Wells

Delft University of Technology, Faculty of Aerospace Engineering,
P.O. Box 5048, 2600 GA Delft, the Netherlands
e-mail: G.N.Wells@citg.TUDelft.nl

Abstract. *Localisation processes, such as shear banding and necking, have been investigated following a macroscopic and a microscopic approach. Both approaches have been formulated within a finite deformation plasticity framework. Additional terms have been used to regularise the problem and solve mesh dependency. In the macroscopic model viscosity is introduced as a means to control the thickness of the shear band, while in the microscopic model the nonlocal interaction of dislocations acts as a stabiliser. The micro-mechanical model is formulated in a crystal plasticity framework. A diffusion term that represents cross-slip of dislocations is included in the evolution equations for dislocation densities. The effect of the viscous term (macro-model) and the diffusion-like term (micro-model) in the constitutive relation on the resulting formation of localised shear modes is studied. An analysis of a strip in tension oriented for multiple slip is presented for both models.*

1 Introduction

The response of mechanical systems at the level of interest is largely determined by processes at scales many times smaller (micro- or meso-level). For this reason, the analysis of the micro- or meso-level mechanisms that determine the deformation and failure behaviour at higher levels is of paramount importance. The analysis of shear banding in crystalline materials involves different length scales. Therefore an attempt is made to perform an analysis of shear banding at two levels: a macro-level at which the material is considered homogeneous and a micro-level with a single crystal structure at which the motion of dislocations cause slip that accumulates in shear banding at a higher level. At both levels a length scale effect is introduced to control the shear band thickness. In this fashion, a bridging of length scales can be established.

First, a macroscopic model is used first for the analysis of shear banding. A von Mises viscoplastic model is formulated in a finite deformation framework. The viscous length scale is introduced to determine the shear band width. The same finite deformation framework is used for a model with a sound micro-mechanical basis. A single crystal plasticity model is chosen, in which shear banding manifests itself by the occurrence of slip lines produced by dislocations in the crystal lattice. A length scale effect is introduced by spatial coupling contributions of the micro-mechanisms. Since dislocations are the true carriers of plastic deformation, gradient plasticity models were formulated in which gradient terms related to dislocation motion were included to account for the spatial interaction, e.g. [4,6,7,11]. In this paper, dislocation glide and cross-slip will be shown to provide a spatial coupling mechanism through a second-order gradient term. The dislocation based gradient plasticity model is outlined in Section 4 for the case of multiple slip in an f.c.c. crystal. The problem to be solved is a coupled problem in which a mechanical equation representing the single crystal model is used together with a reaction-diffusion type equation describing the nonlocal dislocation motion on specific slip systems.

The macroscopic and the microscopic model have been used for the analysis of shear banding in a strip loaded in uniaxial tension. By comparing the thickness of the shear band, the microscopic parameters (dislocation 'diffusivity') can be coupled to the macroscopic parameters (viscosity). Consequently, a length scale effect at macro-level can be given a micro-structural basis.

2 Macroscopic model for localisation

A macroscopic model for the modelling of localisation processes, such as shear banding and necking, is formulated within a finite deformation plasticity framework using the multiplicative decomposition of the deformation gradient $\mathbf{F}$ into an elastic part $\mathbf{F}^e$ and a plastic part $\mathbf{F}^p$

$$\mathbf{F} = \mathbf{F}^e \mathbf{F}^p \ . \tag{1}$$

The plastic part $\mathbf{F}^p$ defines the intermediate configuration. The plastic flow rule is written as

$$\dot{\mathbf{F}}^p (\mathbf{F}^p)^{-1} = \dot{\lambda} \mathbf{n}(\mathbf{S}, \boldsymbol{\kappa}) \ , \tag{2}$$

where λ is the plastic multiplier and $\mathbf{n}$ is the direction of plastic flow. The discretisation of this equation consists of taking the direction of the plastic flow $\mathbf{n}$ constant throughout the increment and equal to its final value $\mathbf{n}_{t+\Delta t}$

$$\dot{\mathbf{F}}^p_{t+\Delta t} = \exp(\Delta \lambda \mathbf{n}_{t+\Delta t}) \mathbf{F}^p_t \ . \tag{3}$$

The elastic response is expressed in terms of a logarithmic elastic strain tensor. The second Piola-Kirchhoff stress tensor is related to the intermediate plastic configuration $\mathbf{S} = \mathbf{F}^{e-1}\tau\mathbf{F}^{e-T}$ (τ is the Kirchhoff stress tensor) which is calculated from the elastic part of the deformation according to

$$\mathbf{S} = \mathbf{S}(\tfrac{1}{2}\log\mathbf{C}^e) \tag{4}$$

where $\mathbf{C}^e = (\mathbf{F}^e)^T\mathbf{F}^e$ is the elastic right Cauchy-Green deformation tensor.

In rate-independent elasto-plasticity the stress state cannot be outside the yield surface defined by the yield function $f(\mathbf{S}, \kappa)$. For isotropic hardening/softening, the yield function, $f(\mathbf{S}, \kappa)$ depends on the history of loading. The plastic multiplier is then determined from the Kuhn-Tucker loading/unloading conditions

$$\dot{\lambda} \geq 0,\ f(\mathbf{S}, \kappa) \leq 0,\ \dot{\lambda}\ f(\mathbf{S}, \kappa)\ =\ 0,\ \dot{\lambda}\ \dot{f}(\mathbf{S}, \kappa)\ =\ 0\ . \tag{5}$$

In the case of viscoplasticity the current stress state can lie outside the yield surface and the Kuhn-Tucker loading/unloading conditions are no longer applicable. The viscoplastic flow is determined by the plastic relaxation equation

$$\dot{\lambda} = \frac{1}{\eta}\,\Phi(\mathbf{S}, \kappa) \tag{6}$$

or in discrete format

$$\Delta\lambda = \frac{\Delta t}{\eta}\,\Phi_{t+\Delta t} \tag{7}$$

where η is a viscosity parameter and the overstress Φ is governed by the yield function, such that $\Phi = 0$ when $f \leq 0$ and $\Phi > 0$ when $f > 0$.

Without loss of generality, we assume a linear isotropic elastic response and having in mind applications for metals a J_2 flow theory is commonly used. This implies associative plastic flow and a von Mises yield function that is given by

$$f(\mathbf{S}, \kappa) = \sqrt{3J_2} - \bar{\sigma}(\kappa)\ . \tag{8}$$

In case of associative plasticity, viscoplastic flow is determined by the gradient of the yield surface

$$\mathbf{n} = \frac{\partial\Phi}{\partial\mathbf{S}} \tag{9}$$

where J_2 is the second invariant of the deviatoric stress and $\bar{\sigma}(\kappa)$ is the yield stress dependent on the equivalent plastic strain κ, which is defined according to

$$\kappa = \int_0^t \dot{\kappa}\,dt\ , \tag{10}$$

and

$$\dot{\kappa} = \sqrt{\frac{2}{3}\,\dot{\boldsymbol{\varepsilon}}^p : \dot{\boldsymbol{\varepsilon}}^p}\ , \tag{11}$$

where $\dot{\boldsymbol{\varepsilon}}^p$ is the viscoplastic strain rate tensor. It can be easily shown that for von Mises plasticity $\dot{\kappa} = \dot{\lambda}$.

3 Numerical examples - macroscopic model

To investigate shear banding with the macroscopic model, a strip in plane strain tension is analysed. A 4 mm by 10 mm strip is pulled by applying a constant axial velocity $v_0 = 0.1$ mm/s at the top and the bottom of the specimen (see Figure 1). The two vertical edges of the strip are traction free. The elastic material parameters for a representative metallic material are as follows: the Young's modulus is 100000 N/mm^2 and Poisson's ratio is 0.3. Von Mises plasticity is used with a linear hardening law according to

$$\bar{\sigma}(\kappa) = \bar{\sigma}_0 + h\kappa , \tag{12}$$

in which the initial yield stress $\bar{\sigma}_0 = 390$ N/mm^2 and the hardening modulus $h = -2000$ N/mm^2. The viscosity parameter η is taken as 0.5 s. In order to trigger shear banding, a small imperfection (reduction of the initial yield stress by 2.5 %) is applied slightly to the right of the centre of the strip (see Figure 1). Three different meshes were used with 320 (mesh 1), 720 (mesh 2) and 1280 (mesh 3) 6-noded triangular elements.
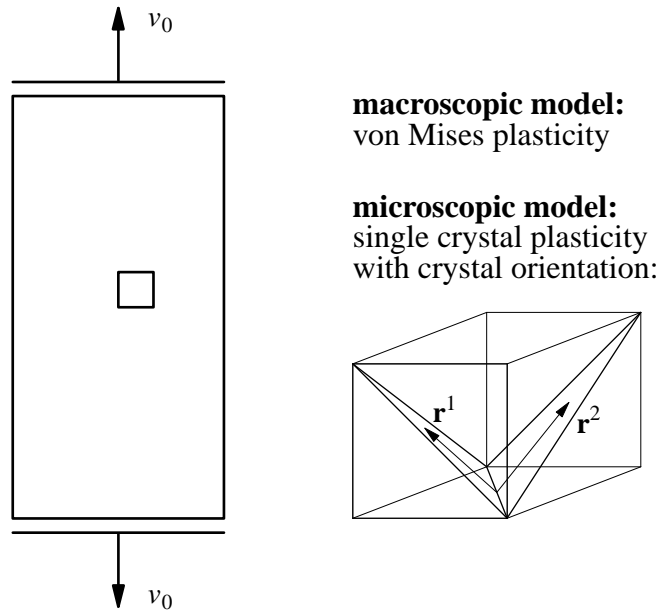

Figure 1. Strip analysed with micro-model and macro-model.

The results after the development of significant shear banding are shown in Figure 2 (deformations are multiplied by a factor of 30). A double shear band emanates from the imperfect zone in the strip. It is clear that the thickness of the band is independent of the size of the finite element. The three different meshes give practically the same results. Viscosity regularises this quasi-static problem. Variation of the viscosity results in a variation of the thickness of the band (see Figure 3). An increase of the viscosity widens the shear band or even prevents localised deformation in the strip. A decrease of viscosity has the opposite effect.
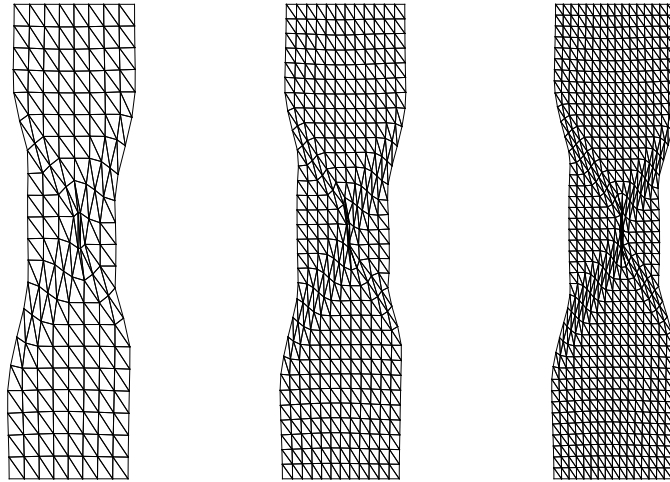
Figure 2. Deformed models (mesh 1,2,3 from left to right) at $t = 0.1$ s.
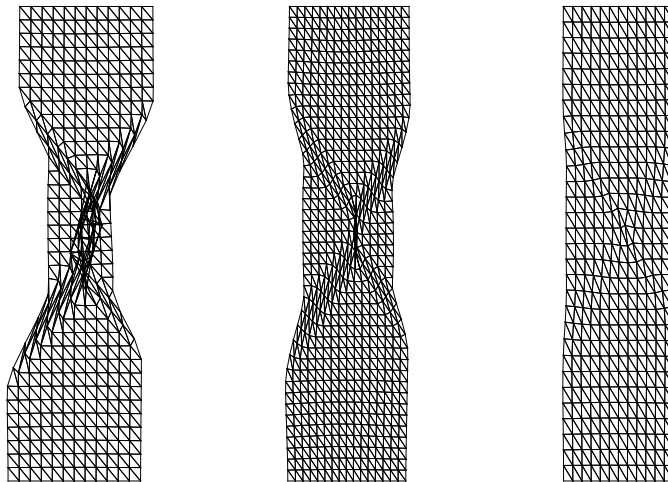

Figure 3. Deformed models (mesh 3) for $\eta = 0.3$ s (left), $\eta = 0.5$ s (centre)
and $\eta = 0.7$ s (right) at $t = 0.1$ s.

4 Microscopic model for localisation

The finite deformation plasticity model discussed in Section 2 is now given a micro-structural basis. The micro-structure is incorporated by considering the metal as a single crystal with hardening behaviour that arises from dislocation density evolution. Deformation of a single crystal is assumed to arise from two main mechanisms: (i) the dislocation motion on active slip systems and (ii) the distortion of the crystal lattice. The kinematic scheme for a finite deformation together with a constitutive formulation for a single crystal is presented e.g. in [1,8].

The multiplicative decomposition of the deformation gradient **F**, cf. eqn(1), is used again,

$$\mathbf{F} = \mathbf{F}^e\mathbf{F}^p , \tag{13}$$

where the elastic part $\mathbf{F}^e$ now describes the stretching and rotation of the lattice and the plastic part $\mathbf{F}^p$ defines the cumulative effect of dislocation motion. A slip system α is specified by the vectors $\bar{\mathbf{s}}^\alpha$ and $\bar{\mathbf{m}}^\alpha$ defined in an intermediate configuration as the corresponding slip direction and slip plane normal, respectively. When the single crystal undergoes deformation, the lattice stretches and rotates and the slip system α in the updated configuration is governed by

$$\mathbf{s}^\alpha = \mathbf{F}^e\bar{\mathbf{s}}^\alpha \tag{14}$$

and

$$\mathbf{m}^\alpha = \bar{\mathbf{m}}^\alpha(\mathbf{F}^e)^{-1} . \tag{15}$$

Since $\bar{\mathbf{s}}^\alpha$ and $\bar{\mathbf{m}}^\alpha$ are orthogonal in the undeformed lattice, so are $\mathbf{s}^\alpha$ and $\mathbf{m}^\alpha$ in the deformed lattice.

Differentiation of eqn(13) gives the velocity gradient

$$\dot{\mathbf{F}}\mathbf{F}^{-1} = \dot{\mathbf{F}}^e(\mathbf{F}^e)^{-1} + \mathbf{F}^e\dot{\mathbf{F}}^p(\mathbf{F}^p)^{-1}(\mathbf{F}^e)^{-1} , \tag{16}$$

in which a superimposed dot denotes the material time derivative. The first and second terms in eqn(16) represent the elastic and the plastic part of the velocity gradient, respectively. Because plastic deformation is assumed to occur only by shearing on the slip systems we have

$$\mathbf{F}^e\dot{\mathbf{F}}^p(\mathbf{F}^p)^{-1}(\mathbf{F}^e)^{-1} = \sum_\alpha \dot{\gamma}^\alpha\mathbf{s}^\alpha\otimes\mathbf{m}^\alpha , \tag{17}$$

with $\dot{\gamma}^\alpha$ denoting the slip strain rate. Using eqns(14) and (15), eqn(17) can be rewritten to yield the flow rule given in [8]

$$\dot{\mathbf{F}}^p(\mathbf{F}^p)^{-1} = \sum_\alpha \dot{\gamma}^\alpha\bar{\mathbf{s}}^\alpha\otimes\bar{\mathbf{m}}^\alpha . \tag{18}$$

We introduce the resolved shear stress on system α, τ^α, which is work conjugate to the slip strain rate $\dot{\gamma}^\alpha$, via

$$\tau^\alpha = \mathbf{s}^\alpha\boldsymbol{\tau}\mathbf{m}^\alpha , \tag{19}$$

where $\boldsymbol{\tau}$ is the Kirchhoff stress (for derivation see e.g. [1]). To relate the rate of shear deformation to the resolved shear stress τ on a slip system α, we make use of a viscous power-law of the form (see e.g. [3])

$$\dot{\gamma}^\alpha = \begin{cases} \dot{\gamma}_0^\alpha\left[(\tau^\alpha/g^\alpha)^{1/m} - 1\right] & \text{if } \tau^\alpha > g^\alpha \\ 0 & \text{otherwise} \end{cases} \tag{20}$$

in which $\dot{\gamma}_0^\alpha$ is a reference shear strain rate, m is the strain rate sensitivity exponent and g^α is the yield stress on slip system α. The hardening of the material is specified by the evolution of the yield stress g^α. A slip system α is considered as active if τ^α is larger than the threshold g^α. In macroscopic hardening models the evolution with time of the yield stress is generally defined in terms of the slip strain rate as

$$\dot{g}^\alpha = \sum_\beta h^{\alpha\beta}\dot{\gamma}^\beta . \tag{21}$$

The strain hardening matrix $h^{\alpha\beta}$ is dependent on internal variables which evolves with γ^β, and local interaction between slip systems with different orientations is taken into account via the off-diagonal terms in $h^{\alpha\beta}$. In the micro-mechanically based model a dependence of $h^{\alpha\beta}$ on the

dislocation density, which plays the role of an internal variable, will be assumed.

The expression for the yield stress is taken in the form [5]

$$g^\alpha = aGb\sqrt{\sum_{\beta \neq \alpha} \rho^\beta} \tag{22}$$

where G is the shear modulus, b is the magnitude of the dislocation Burgers vector, a is a constant and ρ^α is the density of dislocations moving on the slip system α, with $\alpha = 1, 2$ for double-conjugate slip and $\alpha = 1 - 12$ for a face-centred cubic (f.c.c.) crystal. According to eqn(22), the yield stress for one slip system is assumed to be determined by the dislocation density on the other slip systems only. In other words, latent hardening is included while self-hardening of a particular slip system is neglected. Also, the reference shear strain rate $\dot{\gamma}_0$ is related to the dislocation density via

$$\dot{\gamma}_0^\alpha = k\rho^\alpha \quad \alpha = 1, 2, \tag{23}$$

where k is a constant. The evolution of the dislocation density is defined by

$$\dot{\rho}^\alpha = \dot{\gamma}^\alpha(J\sqrt{\rho^\beta} - K\rho^\alpha) + D\nabla^2\rho^\alpha ; \quad \alpha \neq \beta \tag{24}$$

suggesting that the mean free path of dislocations of a slip system is determined by the dislocation density of the other slip system. The recovery process is assumed to involve two dislocations of the same slip system giving rise to the negative term on the right-hand-side of eqn(24). The coefficient J in the athermal dislocation storage term is considered to be a constant while the coefficient K is the thermally activated recovery term, which is generally temperature and strain rate dependent. The *isotropic dislocation diffusion* term in eqn.(24) represents the cross-slip effect. The diffusivity D is determined by the cross-slip frequency of dislocations and the active slip plane spacing. Taking the derivative of (22) with respect to time and making use of eqn.(24) yields the equations from which the hardening matrix can be computed according to

$$h^{\alpha\beta} = \frac{\partial\dot{g}^\alpha}{\partial\dot{\gamma}^\beta} = \begin{bmatrix} \dfrac{\partial\dot{g}^1}{\partial\dot{\gamma}^1} & \dfrac{\partial\dot{g}^1}{\partial\dot{\gamma}^2} \\ \dfrac{\partial\dot{g}^2}{\partial\dot{\gamma}^1} & \dfrac{\partial\dot{g}^2}{\partial\dot{\gamma}^2} \end{bmatrix}. \tag{25}$$

The model presented has the following features. Strain softening associated with local lattice rotation may give rise to strain localisation at later stages of deformation when it can no longer be restrained by strain hardening, cf. [1,2]. In the present model, this effect decreases because of the gradient terms which force the evolving dislocation densities to saturate. Due to the positive sign of D the 'diffusion-like' terms in the equations will act against strain localisation and will thus play a stabilising role. The algorithmic aspects of the model are described in [10].

5 Numerical examples - microscopic model

To investigate the behaviour of the gradient plasticity model for dislocation motion in a single crystal, the strip in tension is considered again (see Figure 1). Multiple slip in a rectangular strip of an f.c.c. crystal is analysed. The crystallographic orientation in the strip is according to an $(\mathbf{a}_1, \mathbf{a}_2, \mathbf{a}_3) = ([1\,0\,\bar{1}],[0\,1\,0],[1\,0\,1])$ coordinate system, which for axial tension results in active slip on the $(11\bar{1})$ plane in the directions $[\bar{1}10]$ and $[011]$ with resultant $\mathbf{r}^1$ and on the $(1\bar{1}\bar{1})$ plane in the directions $[110]$ and $[01\bar{1}]$ with resultant $\mathbf{r}^2$ (see Figure 1). The values for the material constants employed are : $G = 75000$ N/mm^2, $a = 0.3$, $b = 2.5 \cdot 10^{-7}$ mm, $\rho_0 =$

$1 \cdot 10^8$ mm^{-2}, $m = 0.005$, $k = 1/\rho_0$, $K = 10$, $J = 4 \cdot 10^6$ mm^{-1}, $D/\sqrt{\rho_0} = 2$ mm^3/s. As with the macroscopic model a small imperfection was used to trigger shear banding, cf. Section 3 (reduction of constant a by 2.5 %). The meshes described in Section 3 were used again.

The results after a certain amount of crystallographic slip are shown in Figure 4. The deformed models for the three different meshes show that one shear band becomes dominant due to the asymmetric location of the imperfection and the structure of the mesh (deformations are multiplied by a factor of 30). The shear band has a specific thickness which is predominantly set by the material parameters J and D and also by the dimensions of the strip and the boundary conditions. It is obvious that the direction of the shear band is not aligned with the mesh. It runs steeper than 45 degrees.
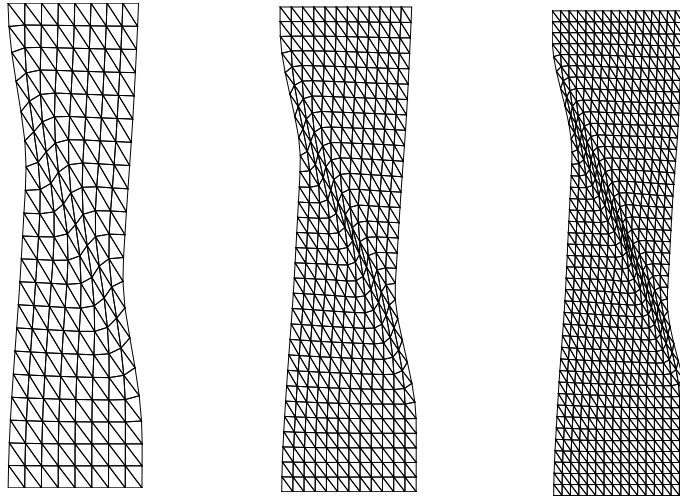

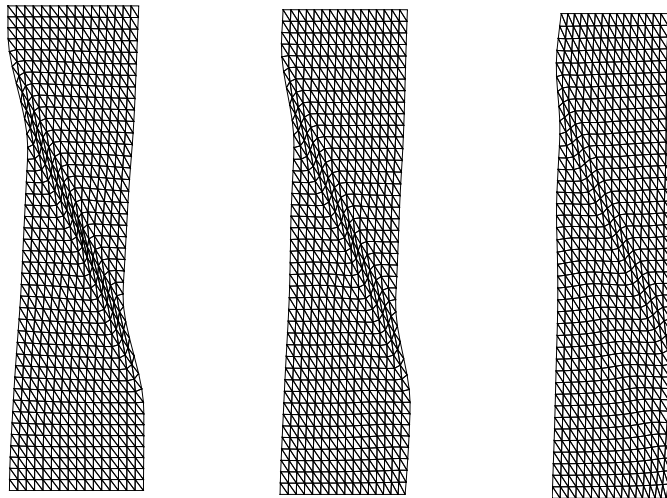Figure 4.   Deformed models (mesh 1,2,3 from left to right) at $t = 0.1$ s.

Figure 5.   Deformed models (mesh 3) for $D/2$ (left), D (centre) and $D \times 2$ (right) at $t = 0.1$ s.

Figure 4 shows the insensitivity of the results to the finite element size. The thickness of the band is slightly overpredicted with the coarsest mesh, but the two finer meshes show the same shear banding process. Next, the amount of coupling is varied through the magnitude of the dislocation diffusivity D. Increasing diffusivity widens the shear band, while a decrease of D leads to a slightly thinner band (see Figure 5).

6   Coupling micro-scale to macro-scale

Analyses at two different scales of observation have been carried out. The introduction of a length scale sets the width of the shear band in the micro-model and the macro-model. The viscous length scale at macro-level is purely phenomenological, while the length scale at micro-level has a micro-mechanical basis. By comparing the width of the shear band in the two finite element computations the macroscopic length scale can be coupled to the microscopic length scale.

In the micro-model the length scale effect is represented by the diffusivity D. The diffusivity is determined by the cross-slip frequency ω and the active slip plane spacing d according to

$$D \;=\; \omega d^2 \; . \tag{26}$$

In the macro-model that is used the viscosity η plays the role of a length scale parameter (see e.g. [9]). By comparing the analyses from Figure 3 with the analyses in Figure 5 a similar shear band thickness is obtained for $D/\sqrt{\rho_0} \;=\; 2 \text{ mm}^3/\text{s}$ and for $\eta \;=\; 0.5$ s. This is a very simple approach and should be seen as a first attempt to give a microscopic argumentation for higher-order terms that are included in macroscopic models. The microscopic model 'informs' the larger scale model on the length scale effect. Two remarks should be made. The comparison which was carried out here was done for one analysis. For a proper coupling between slip plane spacing d (or diffusivity D) and viscosity η more analyses should be carried out. Material parameters and the size of the specimen should be varied. Furthermore, both length scale effects are dependent on the rate of loading. For this reason, tests at different loading rate should be carried out. A second remark is concerned with the failure pattern. Viscous regularisation is slightly stronger than the nonlocal regularisation by dislocation diffusion in the micro-model. For this reason a more symmetric failure pattern is obtained with the macro-model. This makes the coupling of parameters also more difficult.

References

[1]   Asaro, R.J. (1983). Micromechanics of crystals and polycrystals. *Adv. Appl. Mech.* **23,** 2-115.

[2]   Balke, H. and Estrin, Y (1994). Micromechanical modelling of shear banding. *Int. J. Plasticity,* **10,** 133-147

[3]   Cuitiño A.M. and Ortiz M.A. (1992). Computational modelling of single crystals.

Modelling Simul. Mater. Sci. Engng **1,** 225-263.

[4]   Estrin, Y. and Mühlhaus, H.-B. (1996). From micro- to macroscale: gradient models of plasticity. Australian Engineering Mathematics Conference, W.Y.D. Yen, P. Broadbridge and J.M. Steiner, (eds.), Sydney, 161-165.

[5]   Estrin, Y., Sluys, L.J., Brechet, Y. and Molinari, A. (1998). A dislocation based gradient plasticity model. *J. de Physique IV France,* **8,** 135-141.

[6]   Fleck, N.A. and Hutchinson J.W. (1997). Strain gradient plasticity. *Adv. in Applied Mechanics,* ed. Hutchinson, J.W. and Wu, T.T., **33,** 295-361.

[7]   Mühlhaus, H.-B. and Boland, J. (1991). A gradient plasticity model for Lüders band propagation. *PAGEOPH* **137,** 391-407.

[8]   Rice, J.R. (1971). Inelastic constitutive relations for solids: an internal-variable theory and its application to metal plasticity. *J. Mech. Phys. Solids* **19,** 433.

[9]   Sluys, L.J. (1992). Wave propagation, localisation and dispersion in softening solids. Dissertation, Delft University of Technology, Delft.

[10] Sluys, L.J. and Estrin, Y. (2000). The analysis of shear banding with a dislocation based gradient plasticity model. *Int. J. Solids Structures* **37,** 7127-7142.

[11] Walgraef, D. and Aifantis, E.C. (1985). On the formation and stability of dislocation patterns, I-III. *Int. J. Eng. Sci.* **12,** 1351-1372.